

## CHEMICAL AND PHYSICAL STUDY OF WASTE PA2200 POWDER

A. Cristina COSTACHE<sup>1</sup>, Gabriel MOAGĂR-POLADIAN<sup>2\*</sup>, Cosmin A. OBREJA<sup>3</sup>, Oana TUTUNARU<sup>4</sup>, Antonio RĂDOI<sup>5</sup>, Cristina PACHIU<sup>6</sup>

*The paper presents the experimental results regarding the recycling process of waste PA2200 powder resulting from Selective Laser Sintering. This waste refers to that fraction of used powder that is normally vacuum-cleaned and disposed to the dump. This sort of disposal may put a great risk as regards microplastic pollution of the environment. It is the aim of this paper to show a decontamination route that allows recovery of this waste and its further recycling. In this way, a cleaner and more eco-friendly SLS process is obtained. The decontamination process and the detailed characterization of the recovered waste (SEM, EDX, FTIR and Raman spectroscopy) are presented.*

**Keywords:** decontamination, recycling, chemical applications, spectroscopy, structural footprint, microplastic pollution, additive manufacturing

### 1. Introduction

Pollution with plastic became one of the most important problems of today ecosystems. One of its components, the so-called microplastics, presents the greatest risk, being practically ubiquitous in every corner of the Earth planet. This represents one of the greatest challenges as regards the influence of humans on the environment and has dramatic consequences on the biosphere as a whole [1-15]. Because of that, pressure is put on the necessity to adopt novel management and business models at least as regards the manufacturing, use and end-life storage of polymers. Any such approach must be directed towards decreasing the environment footprint of production activity as much as possible.

<sup>1</sup> PhD. Eng., Dept. of Industrial Engineering, Faculty of Industrial Engineering and Robotics, University POLITEHNICA of Bucharest, and National Institute for Research & Development in Microtechnologies, Bucharest, Romania, e-mail: costache.cristina92@yahoo.com

<sup>2</sup> National Institute for Research & Development in Microtechnologies, Bucharest, Romania, e-mail: gabriel.moagar@imt.ro

<sup>3</sup> National Institute for Research & Development in Microtechnologies, Bucharest, Romania

<sup>4</sup> National Institute for Research & Development in Microtechnologies, Bucharest, Romania

<sup>5</sup> National Institute for Research & Development in Microtechnologies, Bucharest, Romania

<sup>6</sup> National Institute for Research & Development in Microtechnologies, Bucharest, Romania

\* Corresponding author: gabriel.moagar@imt.ro

On the other hand, additive manufacturing (AM) is presently developing at a rate currently estimated at 15.0% (CAGR) during the 2015–2025 period [16], due to its application in various industries such as aerospace, automotive, consumer goods. More applications mean more raw material used and more resulting waste. Even if contained in a waste site, this powder presents a high risk of being spread in the environment and thus contributing to the microplastic pollution of it [17-18]. This spread is done mainly by wind and rain. The same considerations apply also for the case of PA2200 particles in water, their sedimentation taking long enough time in order to allow spreading over large distances.

It should be more beneficial to recycle this powder waste and transform it into a raw material, that can be used in other industries such as textile industry, music industry, food industry and personal care.

A first step in the direction of recyclability of this powder waste is the cleaning and decontamination of the wet powder collected from the vacuum cleaner. Two main processes are needed within this first step: removal of dirt and inorganic contaminants (dust); removal of all biological contaminants (bacteria and fungi). These processes are necessary because we work with a material in its powder form. Powders are known to have a very big total surface, meaning that the quantity of contaminants is significant.

The aim of this paper is to present the experimental results obtained so far regarding the PA2200 powder cleaning and decontamination resulting from AM activities at IMT. The accent is put here on the effectiveness of contaminant removal. The priority is represented by the decontamination that allows further powder reuse and, consequently, that leads to avoidance of environment microplastic pollution.

Section 2 presents the recipes and the methodology that were used in the work. Section 3 is devoted to the presentation of the results obtained and to discussions regarding decontamination. The paper ends with the conclusions section.

## 2. Experimental section

### 2.1 Powder source

The powder was extracted from the anti-ex vacuum cleaner used for cleaning the 3D Printing machine, powder bin, other equipment (sieve, blaster) and the 3D Printing laboratory environment, respectively (walls, floor). It is a slurry formed mainly by PA2200 powder with water (from the anti-ex vacuum cleaner) and dust.

In the following figure, there are presented photo and optical microscopy images of nylon powder PA2200 as recovered from the slurry existing inside the vacuum cleaner.

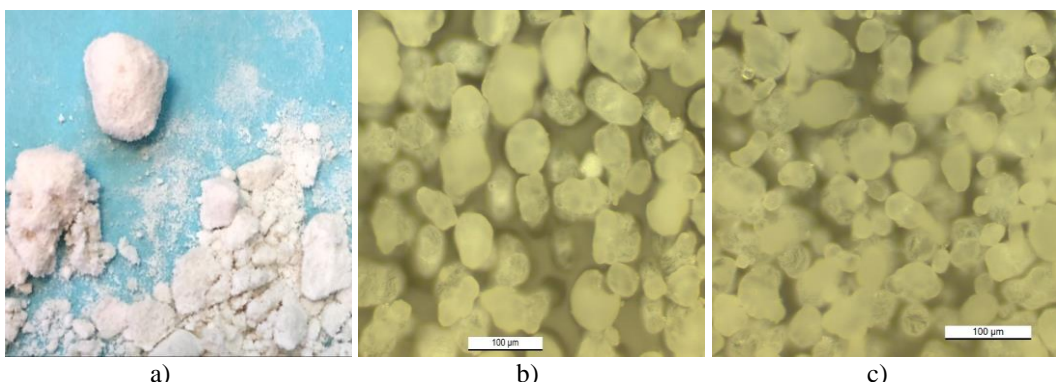


Fig. 1. a) photo image of the powder slurry as extracted from the vacuum cleaner; b) optical microscopy image of the powder from the slurry; c) optical microscopy image of the initial fresh powder

## 2.2 Recipes and methodology

In order to remove inorganic contaminants as best as possible, the following sequence of processes was used. First, the slurry was introduced in a potassium hydroxide solution of various concentration (table 1). We used KOH pills of 99.8 % purity and deionized water when preparing the solution. The solution was heated on a hob under magnetic stirring at temperatures between 60 - 90 ° C, in order to detach the solid particles (usually dust) attached to powder grains and grain aggregates and kept for 2 hours. Then the liquid was let for one day to sediment the insoluble dust part. Secondly, the polymer waste (floating at the solution surface) was taken away from the liquid and introduced into deionized water.

A filter funnel (borosilicate glass 3.3) and a vacuum pump in the washing and filtration process of polymer powder were used. The filter has a porosity that allows the passage of particles having a diameter of 16 microns or less. The purpose of the vacuum pump is to accelerate the process of separating the powder from the suspension.

The aqueous polymer dispersion was washed with deionized water and filtered five times for removing the traces of KOH solution. The suspension remained in the filter funnel, and the KOH was collected in the glass along with the impurities. The washing cycle was repeated 5 times. In the sixth wash step the filtered wet polymer bed was re-dispersed in one liter of deionized water where 50 ml isopropyl alcohol (VLSI degrees, BASF) and 25 ml freshly prepared aqueous 1% hydrochloric acid (Sigma Aldrich, 37%) were added.

For the most effective removal of potassium ions, a dilute hydrochloric acid solution was used to neutralize the polymer dispersion. The pH of the aqueous dispersion after neutralization had a value of 5.5-6, which quite close to

the value of pH of the deionized water. This indicates a proper neutralization of the dispersion.

Isopropyl alcohol has been used for better wetting of polymer grains in water and to improve the removal of potassium ions from the surface of the polymer particles. The traces of isopropyl alcohol also helped to eliminate water during the drying step.

In the drying step, the wet polymer powder was collected into a cylindrical vessel which was subsequently introduced into a vacuum oven (Memert VO400, Germany) at 60 °C for 3 hours, at a vacuum of 30 mbar. The vacuum was quenched with nitrogen and the powder allowed to cool down to room temperature.

KOH was used for several reasons. First, some preliminary experiments on 100 microns thick PA2200 membranes were made to check for any adverse effect of KOH on PA2200. The test was made by partially immersing several such membranes in a 40 % KOH solution at 80°C for a duration of 4 hours. Then, the separation region between the immersed and non-immersed parts was examined at an optical microscope. No visible differences were noticed between the two regions. Another reason for using KOH was that it is a strong base that is able to remove most of the inorganic compounds found on the powder grains surface.

The work plan after which the decontamination was carried out is presented in table 1.

**Table 1**  
**Test conditions and sets for decontamination of nylon powder**

Set of tests Conditions	C1	C2	C3	Drying time in the oven (h)
Set 1	C <sub>KOH</sub> =40%	T= 80°C	t = 2h	3h; T= 60°C
Set 2	C <sub>KOH</sub> = 40%	T= 60°C	t = 2h	
Set 3	C <sub>KOH</sub> = 40%	T= 90°C	t = 1h	
Set 4	C <sub>KOH</sub> = 20%	T= 80°C	t = 2h	
Set 5	C <sub>KOH</sub> = 20%	T= 60°C	t = 2h	
Set 6	C <sub>KOH</sub> =60%	T= 80°C	t = 1h	
Set 7	C <sub>KOH</sub> =60%	T= 60°C	t = 1h	

First, we analyzed the first set of tests - set 1. Second, for the following test sets we varied the KOH concentration was varied (Condition C1), temperature (Condition C2), and the heating time (Condition C3).

### 2.3 Physical characterization

The set of tests consisted in the characterization of the cleaned powder with respect to the used powder (as recovered from the anti-ex vacuum cleaner) and fresh powder. The reason for this second set of tests is to determine whether

or not the decontamination process affects the structure and composition of the powder. For this purpose, we have used the following equipment: FEI Nova Nano SEM 630 for performing scanning electron microscopy, Element EDS system for EDX, Bruker Vertex 80 v (Tensor 27/Bruker Optics) spectrometer for FTIR and, respectively, WITec RAMAN spectrometer alpha 300S for Raman spectroscopy.

### 3. Results and discussions

#### 3.1. Results

SEM and EDX were used to characterize the surface morphology and the composition of the PA2200 samples. The SEM images were obtained using a TLD detector, an acceleration voltage of 15 kV and a working distance of about 5 mm.

The SEM micrographs of the reference, contaminated and decontaminated powder sample, are presented in Fig. 2. Each column of two photos corresponds to one of these samples.

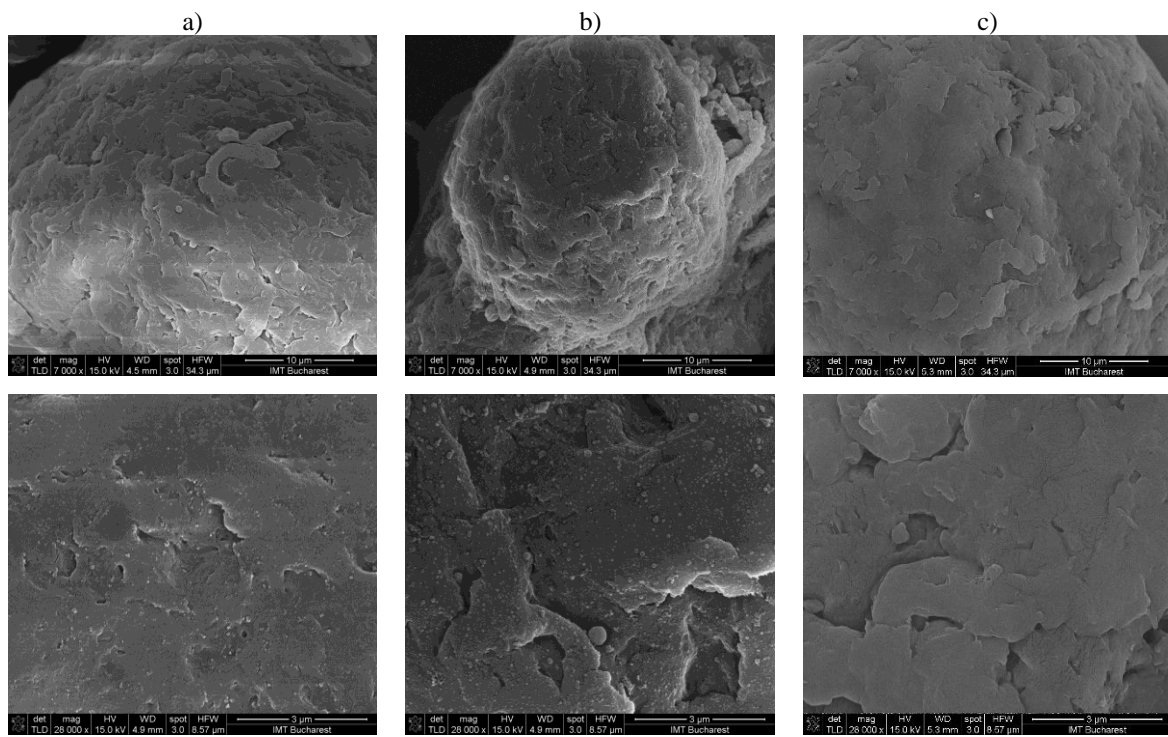


Fig. 2. SEM micrograph of the: a) reference; b) contaminated; c) decontaminated powder sample having different magnification (7kx top images, 28kx lower images)

In the reference sample we can observe a few nanoparticles of about 50 nm; furthermore, in the contaminated samples we can remark a multitude of nanoparticles in the range of 70-430 nm. In the decontaminated sample the

nanoparticles are not present due to KOH solutions. This is due to the fact that the poorly fixed nanoparticles that were at the surface of the sample were removed during the decontamination treatment and passed through the filters used in the experiment. Moreover, a slight etching of the polymer might have happened, as results from the comparison between Figs. 2a and 2c, respectively. The surface of the decontaminated sample is a little bit smoother than the surface of the reference powder, suggesting a slight etching at the powder grain surface. Another important observation is that the contaminated powder has a rougher surface than the fresh one, aspect that is specific to polymer SLS. This rougher surface offers a better fixing of contaminants, considering its shape and the presence of polar groups in PA2200 molecule. The chemical constituents of interest within the PA2200 sample were revealed by the EDX spectra at 4kx magnification. From the EDX spectra we noticed different concentrations of Carbon, Nitrogen and Oxygen. We can notice a difference between the concentration of Nitrogen and Oxygen from the reference to the contaminated sample (see table 2):

**Table 2**  
**Elemental composition of the polymer powder sets as resulted from EDX analysis**

Element	Weight %			Atomic %			Net Intensity		
	Ref	Cont	Decont	Ref	Cont	Decont	Ref	Cont	Decont
C	67.98	72.28	69.96	72.96	77.48	74.93	272.36	264.42	278.42
N	10.87	6.76	8.01	10.01	6.21	7.36	7.70	4.32	5.47
O	21.15	19.49	22.03	17.04	15.69	17.71	32.45	29.25	34.32
Si	-	0.37	-	-	0.17	-	-	1.03	-
P	-	0.78	-	-	0.32	-	-	1.69	-
S	-	0.31	-	-	0.12	-	-	0.62	-

These differences are most probably due to the contaminants existing on the surface of the respective sample. Also, we can observe that the reference sample is not that different from the decontaminated sample. More details can be observed in Fig. 3.

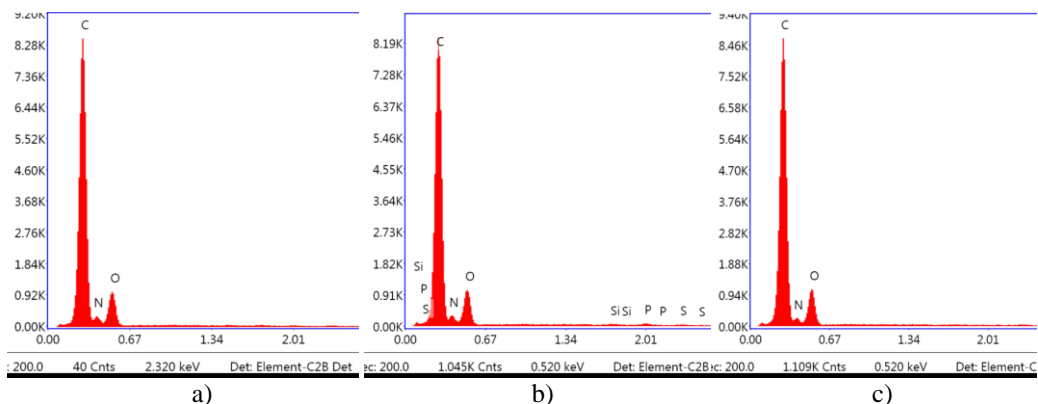


Fig. 3. EDX spectrum of the reference (a), contaminated (b) and decontaminated samples (c)

It is observed from the EDX spectra that the contaminated powder contains also Si, P and S. While Si can be ascribed to the mineral component of dust ( $\text{SiO}_2$ ), P can be ascribed both to the organic contaminant and to a phosphate-based component of the mineral fraction. Similar consideration can be made for the S component. What is important to see from the EDX analysis is that the decontaminated powder has no contaminant, at least within the detection limit of the EDX system (0.5 % at, resolution 129.2 eV).

FTIR spectra of reference, contaminated and decontaminated PA2200 powders are illustrated in Fig. 4 and peak assignment is reported in Table 3:

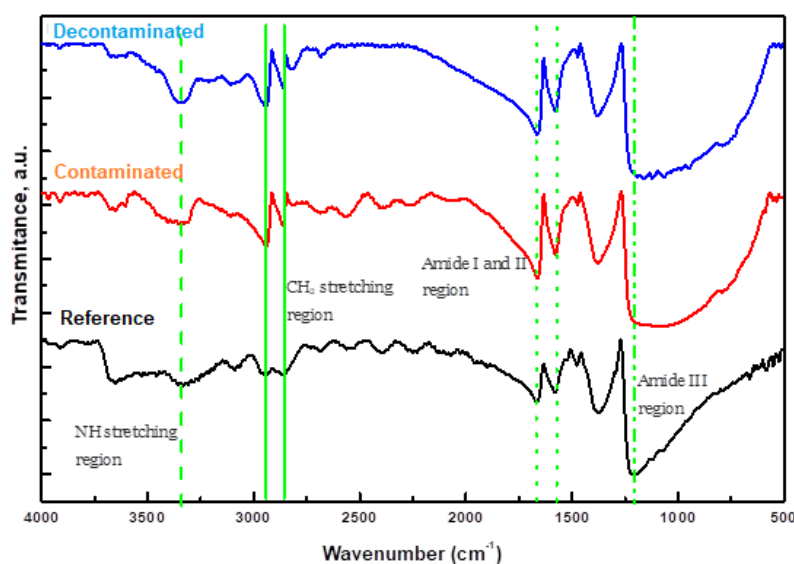


Fig. 4. FTIR spectra of pristine, waste and recovered PA2200 powders

Table 3

**FTIR assignment of reference, contaminated and decontaminated PA2200 powders**

Reference PA2200		Contaminated PA2200		Decontaminated PA2200	
Position (cm <sup>-1</sup> )	Peaks assignment	Position (cm <sup>-1</sup> )	Peaks assignment	Position (cm <sup>-1</sup> )	Peaks assignment
3358	N–H stretching	3352	N–H stretching	3354	N–H stretching
2945	Asymmetric and symmetric stretching of $\text{CH}_2$	2941	Asymmetric and symmetric stretching of $\text{CH}_2$	2941	Asymmetric and symmetric stretching of $\text{CH}_2$
2860		2862		2860	
1666	Amide I absorption band	1663	Amide I absorption band	1664	Amide I absorption band
1581	Amide II absorption band	1577	Amide II absorption band	1577	Amide II absorption band
1475	$\text{CH}_2$ bending, CH bending and $\text{CH}_2$ twisting vibrations	1471	$\text{CH}_2$ bending, CH bending and $\text{CH}_2$ twisting vibrations	1473	$\text{CH}_2$ bending, CH bending and $\text{CH}_2$ twisting vibrations
1375		1377		1379	
1213	Amide III	-	-	1192	Amide III

	absorption band				absorption band
1160	Skeletal motion of CONH	1165	Skeletal motion of CONH	1161	Skeletal motion of CONH
1122	C-C stretching	1084	C-C stretching	1122	C-C stretching

The FTIR spectra revealed the presence of functional groups (-NH, -C=O, -CH<sub>2</sub>-, etc.) ascribable to polyamide. It is worth mentioning that observable modification in spectra was below 1100 cm<sup>-1</sup>, mainly involving amide III groups of the polymer, being known that amide side groups of polyamide are chemically active during SLS.

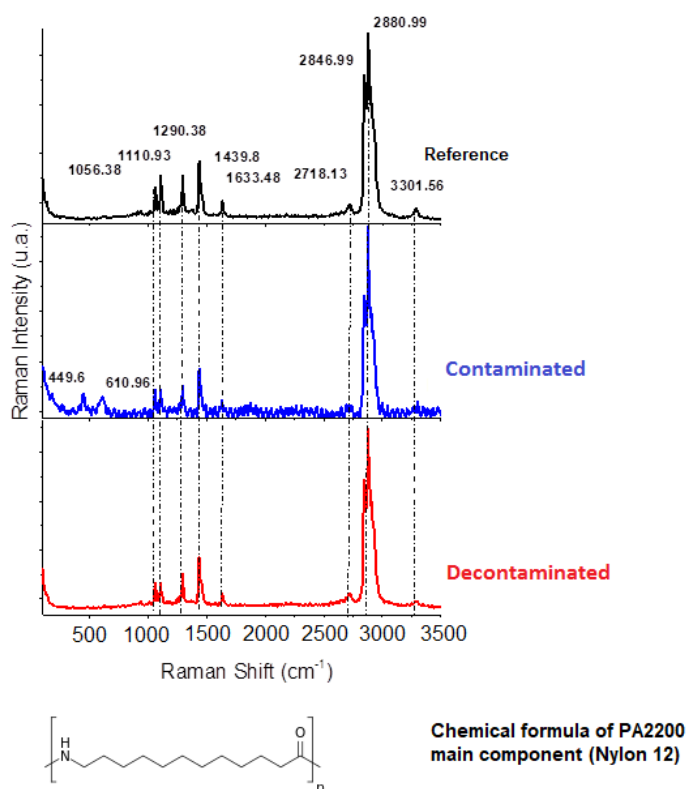


Fig. 5. Raman spectra of reference, contaminated and decontaminated PA2200 powders.

Table 4  
Raman spectra assignment of reference, contaminated and decontaminated PA2200 powders

Assigment	Reference Wave number (cm <sup>-1</sup> )	Contaminated Wave number (cm <sup>-1</sup> )	Decontaminated Wave number (cm <sup>-1</sup> )
Si-O-Si bending ( $\delta$ -bend or R-band)	-	449.6	-
Si-O (D <sub>2</sub> band) <sup>(*)</sup>	-	610.96	-
C-C-O stretch	1059.54	1063.49	1056.38

C-C skeletal stretch	1110.93	1107.76	1110.93
CH <sub>2</sub>	1290.38	1290.38	1290.38
CH <sub>2</sub> aliphatic groups	1436.64	1436.64	1439.8
N-H Amine groups I	1639.81	1636.65	1633.48
CH <sub>2</sub> aliphatic groups	2725.25	2721.29	2718.13
CH <sub>2</sub>	2838.2	2840.67	2846.99
CH <sub>2</sub>	2884.15	2880.99	2880.99
N-H stretch /Amine groups II	3284.17	3288.13	3301.56

(\*) This band allows us to say the 610.96 cm<sup>-1</sup> peak is solely due to SiO<sub>2</sub>.

The most part of the identified groups are ascribable to polyamide. This means that, within the detection limit of the system, the chemistry of the material was not altered by the decontamination process. Some slight differences (as regards position of lines) appear between pristine and contaminated, respectively decontaminated, ones. This shift may be due to the effect of heat during the SLS process through which the contaminated sample has passed. Also, the presence of additional lines in the contaminated sample is an indicator for the presence of SiO<sub>2</sub>, most probably from dust particles. The presence of Si is supported also by the EDX spectra, while the Raman data show the compound in which Si is found.

Based on the FTIR and Raman data, we may affirm that the decontamination process did not changed the chemical composition of the PA2200 powder.

### 3.2 Discussions

First, we underline that we have considered the avoidance of pollution with microplastic particles that have a size of well below 100 microns that are resulting from polymer SLS fabrication process. As is known [20, 21], this is the most difficult microplastic fraction to be removed from waste water. This avoidance is achieved directly at the microplastic source, i.e. the slurry existing in the anti-ex vacuum cleaner. This prevents any environment contamination because of the microplastic transportation to recycling site. Successful decontamination of the powder recovered from the vacuum cleaner offers the possibility of further converting this waste into a material useful in other polymer production processes or other industries. The overall decontamination scheme used for this work is presented in Fig. 6.

We pursued all the decontamination steps up to the drying of the powder, since we were interested only in the decontamination of PA 2200 polymer powder. In order to avoid any further microplastic contamination, the dried powder has to be melted, forming a bulky, solid material piece.

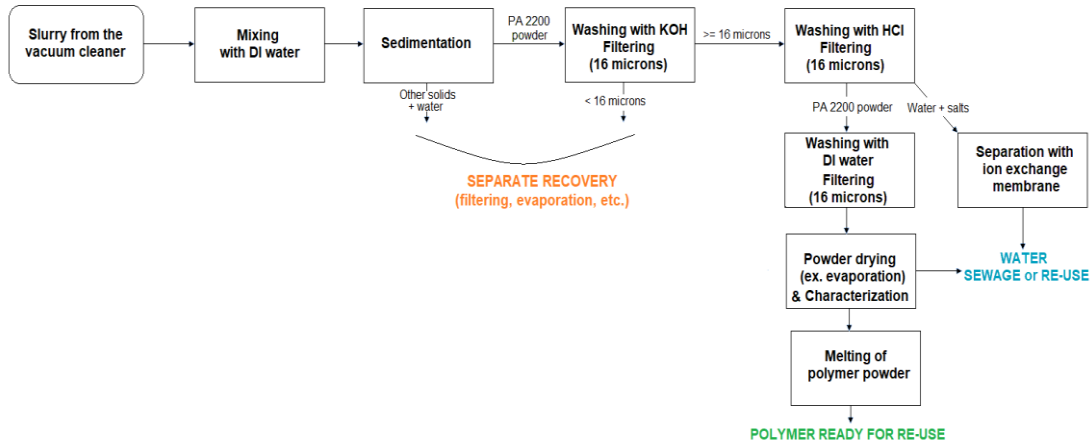


Fig. 6. The decontamination scheme

### 3.2.1 Recovered microplastic cycle

The overall powder cycle used in this work for recovery purposes is depicted in Fig. 7, where the part considered in our work is also presented:

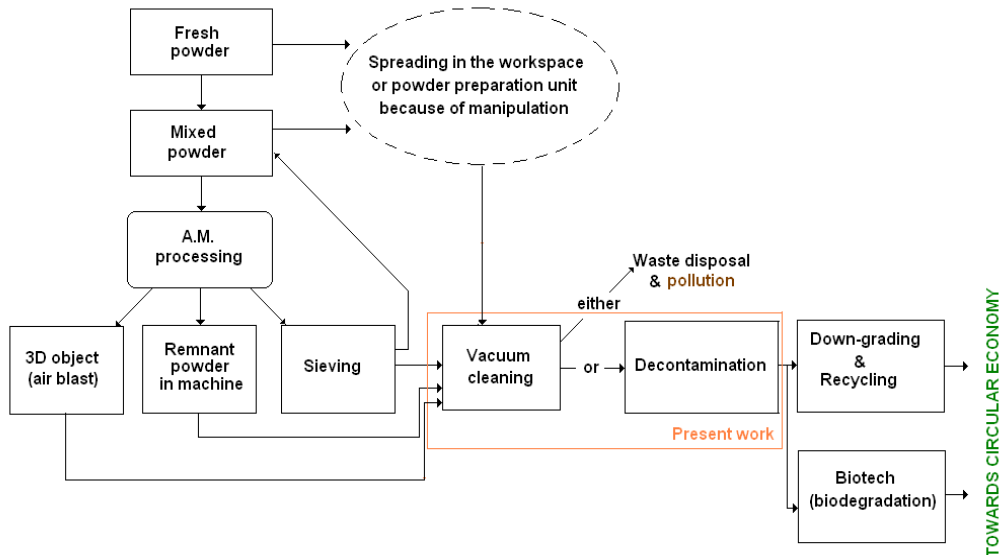


Fig. 7. – The overall powder cycle in polymer SLS

We restricted our experiments to the waste part resulting from the anti-ex vacuum cleaner since it represents the most part (>99.9 %) of the microplastic waste resulting from polymer SLS.

Once decontaminated, the powder is ready for further use. As is known, the recovered polymer has a slightly changed composition as compared to the

fresh powder mainly because of solvent evaporation during SLS process. Moreover, the part obtained from vacuum cleaner contains also polymer multi-particle aggregates that remained above the sieve during the sieving of the powder that passed through SLS. Whichever the route, the microplastic waste is recovered and microplastic pollution prevented.

After the 3D object is taken off from the AM machine, it is first brushed above the sieve for eliminating most of the powder still existing on it, after which it is air blasted in order to clean it as best as possible. Even so, there is some powder remaining on it. Because of that, a third powder removal step is achieved by brushing the object under a water jet.

#### 4. Conclusions

We have identified a potential threat from the waste resulting from polymer SLS systems, waste that is represented by the used PA2200 polymer powder collected into the vacuum cleaner after finishing a SLS process. This powder is of no more use and is usually sent to garbage. We found a way to recover and decontaminate this type of powder waste in order to prevent environmental microplastic contamination with it. The recovering is made just at the source of microplastic.

Chemical and physical characterization showed that no significant etching or chemical reaction had occurred at the surface of the powder grains.

The powder recovered this way may be further melt and re-used. This means that the decontaminated powder can be used in further production processes for making various goods. The decontamination route gives rise to almost zero pollution provided that is correctly applied. Considering and applying such a decontamination route offer the possibility for additive manufacturing to further improve its capabilities as a green industrial technology.

#### Acknowledgements

This work has been funded by the European Social Fund from the Sectoral Operational Programme Human Capital 2014-2020, through the Financial Agreement with the title "Scholarships for entrepreneurial education among doctoral students and postdoctoral researchers (Be Entrepreneur !)", Contract no. 51680/09.07.2019 - SMIS code: 124539.

A.C.C. gratefully acknowledges the support received from Professor Cristian V. Doicin from Faculty of Industrial Engineering and Robotics, University POLITEHNICA of Bucharest, Romania.

## R E F E R E N C E S

- [1] *E. Y. Zeng (ed.)* - “Microplastic Contamination in Aquatic Environments - An Emerging Matter of Environmental Urgency”, Elsevier, ISBN 978-0-12-813747-5, 2018
- [2] *Rachel Hurley, Jamie Woodward, James J. Rothwell* – “Microplastic contamination of river beds significantly reduced by catchment-wide flooding”, *Nature Geoscience* volume 11, p. 251–257, 2018
- [3] *F.A.O.* - “The State of World Fisheries and Aquaculture 2016,” in *Contributing to Food Security and Nutrition for All*, Rome, 2016
- [4] *B. Stephens, P. Azim, Z. El Orch, T. Ramos* – “Ultrafine particle emissions from desktop 3D printers”, *Atmospheric Environment*, Volume 79, p. 334-339, 2013
- [5] *P. Sherman, E. van Sebille* – “Modeling marine surface microplastic transport to assess optimal removal locations”, *Environ. Res. Lett.* **11** 014006, 2016
- [6] *Weimin Wu et al* – “Microplastics pollution and reduction strategies”, *Frontiers of Environmental Science & Engineering* vol. 11(1), 2017, DOI: 10.1007/s11783-017-0897-7
- [7] *Anthony L. Andrade* – “Microplastics in the marine environment”, *Marine Pollution Bulletin*, vol. 62, no. 8, p. 1596-1605, 2011
- [8] *Francesca De Falco et al* – “The contribution of washing processes of synthetic clothes to microplastic pollution”, *Scientific Reports* vol. 9, Article number: 6633, 2019
- [9] *Marcus Eriksen et al* – “Microplastic: What Are the Solutions?”, in: *Wagner M., Lambert S. (eds) Freshwater Microplastics. The Handbook of Environmental Chemistry*, vol 58. Springer, Cham, p. 273-298, 2017
- [10] <https://oceanservice.noaa.gov/facts/microplastics.html>, accessed on October 15, 2019
- [11] *Chelsea M. Rochman et al* – “Microplastics research—from sink to source”, *Science*, vol. 360, no. 6384, p. 28-29, 2018
- [12] *S. Gionfra* – “Plastic pollution in soil”, *Institute for European Environmental Policy*, 2018, <https://ieep.eu/uploads/articles/attachments/3a12ecc3-7d09-4e41-b67c-b8350b5ae619/Plastic%20pollution%20in%20soil.pdf?v=63695425214>
- [13] *S. Sharma, S. Chatterjee* – “Microplastic pollution, a threat to marine ecosystem and human health: a short review”, *Environ. Sci. Pollut. Res Int.*, vol. 24, no. 27, p. 21530-21547, 2017, doi: 10.1007/s11356-017-9910-8
- [14] *R. E. McNeish et al* – “Microplastic in riverine fish is connected to species traits”, *Scientific Reports*, vol. 8, Article number: 11639, 2018
- [15] *K. D. Cox et al* – “Human Consumption of Microplastics”, *Environ. Sci. Technol.*, vol. 53, no. 12, p. 7068-7074, 2019
- [16] *Frost & Sullivan's Global 360° Research Team* – “Global Additive Manufacturing Market, Forecast to 2025”, 2016, [http://namic.sg/wp-content/uploads/2018/04/global-additive-manufacturing-market\\_1.pdf](http://namic.sg/wp-content/uploads/2018/04/global-additive-manufacturing-market_1.pdf), accessed on 19 September, 2019
- [17] *J. Datta et al* – “A New Approach to Chemical Recycling of Polyamide 6.6 and Synthesis of Polyurethanes with Recovered Intermediates”, *Journal of Polymers and the Environment*, vol. 26, p. 4415–4429, 2018
- [18] *S. Swar, V. Zajcova, J. Mullerova, P. Subrtova, J. Horakova, B. Dolensky, M. Rezanka, I. Stibor* - "Effective poly(ethylene glycol) methyl ether grafting technique onto Nylon 6 surface to achieve resistance against pathogenic bacteria *Staphylococcus aureus* and *Pseudomonas aeruginosa*”, *Journal of Materials Science*, vol. 53, p. 14104–14120, 2018.